

pubs.acs.org/JPCB Article

Relevance of Surface Adsorption and Aqueous Complexation for the Separation of Co(II), Ni(II), and Fe(III)

Pan Sun, Erik A. Binter, Trung Vo, Ilan Benjamin, Mrinal K. Bera, Binhua Lin, Wei Bu,* and Mark L. Schlossman*



ACCESS I

Cite This: J. Phys. Chem. B 2023, 127, 3505-3515



Article Recommendations

III Metrics & More : DHDP : HDEHP or HEHEHP Water-soluble extractant Water-insoluble extractant

ABSTRACT: During the solvent extraction of metal ions from an aqueous to an organic phase, organic-soluble extractants selectively target aqueous-soluble ions for transport into the organic phase. In the case of extractants that are also soluble in the aqueous phase, our recent studies of lanthanide ion-extractant complexes at the surface of aqueous solutions suggested that ionextractant complexation in the aqueous phase can hinder the solvent extraction process. Here, we investigate a similar phenomenon relevant to the separation of Co(II), Ni(II), and Fe(III). X-ray fluorescence near total reflection and tensiometry are used to characterize ion adsorption behavior at the surface of aqueous solutions containing water-soluble extractants, either bis(2-ethylhexyl) phosphoric acid (HDEHP) or 2-ethylhexylphosphonic acid mono-2-ethylhexyl ester (HEHEHP), as well as adsorption to a monolayer of water-insoluble extractant dihexadecyl phosphoric acid (DHDP) at the aqueous-vapor interface. Competitive adsorption of Ni(II) and Fe(III) utilizing either HDEHP or DHDP illustrates the essential feature of the recent lanthanide studies that the ion, which is preferentially extracted in liquid-liquid extraction, Fe(III), is found preferentially adsorbed to the water-vapor interface only in the presence of the water-insoluble extractant DHDP. A more subtle competition produces comparable adsorption behavior of Co(II) and Ni(II) at the surfaces of both HDEHP- and HEHEHP-aqueous solutions in spite of the known preference for Co(II) under solvent extraction conditions. Comparison experiments with a monolayer of DHDP reveal that Co(II) is preferentially adsorbed to the surface. This preference for Co(II) is also supported by molecular dynamics simulations of the potential of mean force of ions interacting with the soluble extractants in water. These results highlight the possibility that complexation of extractants and ions in the aqueous phase can alter selectivity in the solvent extraction of critical elements.

1. INTRODUCTION

The application of cobalt and nickel in batteries and electronic devices has increased substantially in the past decades.^{1,2} Efficient extraction and separation from natural ores or electronic waste is paramount for the supply of Co and Ni, yet this separation of neighboring elements is challenging.^{3,4} Liquid-liquid solvent extraction is often used for their separation and purification.⁵⁻⁷ During the extraction process, metal ions are selectively transported across the liquid-liquid interface with the assistance of organic extractant molecules.8 Understanding the role of both bulk and interfacial complexation in the solvent extraction process will help to design and develop new methodologies which enhance the efficiency and selectivity of their separation.

Solvent extraction methods for separating Co(II) from Ni(II) usually extract Co(II) while leaving Ni(II) in the aqueous phase, though some are capable of preferentially extracting Ni(II). The relevant extractants can be divided into three categories based on their extraction mechanism: (1) organophosphorus extractants that utilize cation exchange,

Supporting Information

Received: November 30, 2022 Revised: March 28, 2023 Published: April 5, 2023





Chart 1. Extractant Molecular Structures: (A) HDEHP, (B) HEHEHP, (C) DHDP

such as the HDEHP⁹ and HEHEHP¹⁰ that are studied here (also known, respectively, as P204 and P507), as well as Cyanex 272,¹¹ Cyanex 301 and Cyanex 302,¹² (2) quaternary ammonium salt extractants that utilize anion exchange, such as Aliquat 336 chloride and Cyphos IL 101,^{13,14} and (3) LIX63 that utilizes chelate extraction. Extractants that utilize cation- or anion-exchange preferentially extract Co(II) over Ni(II), while preferential extraction of Ni(II) occurs with chelate extractants.

Early studies of solvent extraction suggested that the complexation of extractant with metal ions takes place either at the interface or in the region near the interface. Paccent studies have used X-ray and neutron scattering and nonlinear optical techniques to probe ion—extractant complexes at liquid surfaces and interfaces. Although the importance of complexation in the bulk aqueous solution had been dismissed in earlier work, other studies have investigated the aqueous solubility of organophosphorous extractants, the influence of this solubility on the extraction process, and the formation of ion—extractant aggregates in the aqueous phase. The low solubility of these extractants in the aqueous phase suggests that they have their greatest effect when ion concentrations are low.

Our recent studies of lanthanide ion complexation with HDEHP in the bulk aqueous phase noted that such complexation can be antagonistic to the intended selectivity of the extraction process.³⁴ The extractant HDEHP is used to preferentially extract heavy over light lanthanides from aqueous to organic phases. Nevertheless, some fraction of the heavy lanthanides remains in the water and some fraction of the light lanthanide is extracted into the organic phase even when the liquid-liquid extraction process proceeds to equilibrium. Multiple species of ions coordinated to water or to extractants contribute to equilibrium partitioning between the liquid phases. Our recent work suggested that bulk complexation in the aqueous phase can contribute to this equilibrium partitioning in a way that opposes the intended separation of heavy lanthanides into the organic phase. Heavy lanthanides can be held back in the bulk water by water-soluble extractants such as HDEHP because they form aqueous ion-extractant complexes whose structure is different from those found in the organic phase. This is analogous to the use of aqueous complexants such as DTPA (diethylenetriamine penta-acetic

acid) that are designed to hold back actinides in the aqueous phase, while lanthanides are extracted into the organic phase in the TALSPEAK process to separate actinides and lanthanides.³⁵ However, aqueous complexants are designed to keep ions in the bulk aqueous phase, whereas extractants dissolved in water can sequester ions in the bulk phase or move ions to the interface.³⁴ An understanding of the role of aqueous complexation can be used to tune extractant selectivity.

Here, we extend our results from the trivalent lanthanides to divalent transition elements Co(II) and Ni(II). In making this extension, we first compare trivalent Fe(III) to Ni(II). Based upon the strong preference for Fe(III) over Ni(II) in solvent extraction processes that utilize HDEHP, it is expected that Fe(III) interacts more strongly with HDEHP.³⁶ This trivalent/ divalent pairing illustrates the role of bulk aqueous complexation on the availability of ionic species at the surface, where we find a predominance of the more weakly interacting Ni(II). Then, we address the smaller differences in interactions displayed by Co(II) and Ni(II) with different extractants. Two soluble extractants were investigated: phosphoric acid HDEHP and phosphonic acid HEHEHP. It is known that HEHEHP exhibits lower extraction efficiency but higher selectivity for Co(II) than HDEHP.³⁷ Our results show a nearly equal presence of these ions at the surface of aqueous solutions of soluble extractants, whereas preferential adsorption of Co(II) is observed when a water-insoluble phosphoric acid extractant (DHDP) is present as a monolayer at the surface. Metal ions with stronger affinity to a water-soluble extractant are sequestered in the bulk of the aqueous solution yet will be found predominantly at the surface when the extractant is confined there. These results suggest the advantage of interfacial interactions for solvent extraction and the disadvantages associated with extractant solubility in the aqueous phase.34

2. METHODS

2.1. Materials. Ultrapure water from a Millipore system with a resistivity of 18.2 $M\Omega$ ·cm was used for all aqueous solutions. Bis(2-ethylhexyl)-phosphoric acid (HDEHP, after purification, >99.9%, Chart 1A) and 2-ethylhexylphosphonic acid mono-2-ethylhexyl ester (HEHEHP, after purification, >99.9%, Chart 1B) were purchased from Alfa Aesar (97%) and

purified via a third-phase formation procedure. ³⁸ FeCl₃·6H₂O (99.99%), CoCl₂·6H₂O (99.9%), and NiCl₂·6H₂O (99.9%) were purchased from Sigma-Aldrich and used without further purification. Dihexadecyl phosphoric acid (DHDP, >98% purity from Avanti Polar Lipids, Inc., Chart 1C) was used without further purification. Sodium hydroxide (NaOH, 98%) was purchased from Alfa Aesar. Hydrogen chloride (HCl, 36.5 to 38.0%) was purchased from Fisher Chemical. Dihexadecyl phosphoric acid (DHDP) was predissolved in chloroform purchased from Sigma-Aldrich (99.9%) to prepare a spreading solution.

2.2. Liquid—**Liquid Solvent Extraction Experiments.** Solvent extraction experiments were performed by pouring 10 mL of organic phase (0.5 mM HDEHP or HEHEHP in dodecane) on top of 10 mL of aqueous phase (0.1 mM Co(II) and 0.1 mM Ni(II)) in a glass centrifuge tube. The mixed two-phase system was shaken with a vortex mixer for 30 min and then centrifuged to obtain a clear separation of two phases. This should produce an equilibrium distribution of ions in the two phases. The concentrations of Co(II) and Ni(II) in the aqueous solution before and after extraction were measured by Inductively coupled plasma-optical emission spectrometry (ICP-OES) (with typical uncertainties of 10%). The extraction percentage of ions and their separation factor were calculated according to the following equations

$$E = \frac{C_0 V_1 - C_1 V_1}{C_0 V_1} \times 100\% \tag{1}$$

$$D = \frac{C_2}{C_1} = \frac{(C_0 V_1 - C_1 V_1) / V_2}{C_1}$$
 (2)

$$\beta = \frac{D_1}{D_2} \tag{3}$$

where E is the extraction percentage of ions, C_0 is the concentration of ions (e.g., Co(II) or Ni(II)) in the aqueous solution before extraction, C_1 is the concentration of the same ion in the aqueous solution after extraction, C_2 is the concentration of the same ion in the organic solution after extraction, V_1 is the volume of the aqueous solution, V_2 is the volume of the organic phase, D is the distribution coefficient of ions, and B is the separation factor between ion 1 and ion 2, where D_1 is the distribution coefficient D of ion 1 and D_2 is the distribution coefficient D of ion 2.

2.3. Preparation of Saturated HDEHP- and HEHEHP-Aqueous Solutions. Aqueous solutions of HDEHP and metal chlorides (CoCl₂, NiCl₂, FeCl₃) were prepared at four different values of pH: 3.5, 4.5, 5.0, and 5.5. Saturated HDEHP- and HEHEHP-aqueous stock solutions were prepared by adding 2 g of HDEHP or HEHEHP into 2 L water and mixing for 30 min. Solutions were allowed to phaseseparate for at least 24 h and then filtered twice through Omnipore filter paper (pore size of 0.2 μ m) to obtain clear solutions. The concentrations of extractant in the saturated stock solutions were measured to be 300 μ M for HDEHP and 180 µM for HEHEHP by ICP-OES. HDEHP and HEHEHP solutions used in our experiments were prepared by diluting the saturated stock solutions by a factor of 15 for HDEHP and by a factor of 8 for HEHEHP with pure water to yield solutions of concentration 20 \pm 1 μ M for HDEHP and 22.5 \pm 1 μ M for HEHEHP as measured by ICP-OES. Then, an appropriate volume of 1 mM metal chloride aqueous solution

was added into the diluted HDEHP- or HEHEHP-aqueous solution to produce a ratio of extractant to each metal ion of 18:1. After that, the pH was adjusted with NaOH or HCl. Metal chloride species are expected to make up a small fraction of the solution as shown in SI Figure S1.

- **2.4. Surface Tension Measurements.** The surface tension of HDEHP and HEHEHP solutions containing different metal ions was measured with the Wilhelmy plate method using a KSV NIMA tensiometry balance with a filter paper plate (Whatman Chr Grade 1 with a width of 1 cm). A Wilhelmy plate (pre-equilibrated with pure water) was lowered to touch the surface of the aqueous solution within a few seconds of pouring the solution into the trough. This defined t = 0 in our time-dependent tension measurements (Figure S3). Equilibrium values of surface tension are reported in this paper.
- **2.5. DHDP Monolayer Preparation.** For the DHDP monolayer experiments, the monolayer was formed by spreading a DHDP-chloroform solution on the surface of aqueous solutions containing different ions, then compressed by a barrier to maintain a constant surface pressure of 10 mN/m. It has been demonstrated that the type of metal ion and aqueous pH are crucial to maintain a stable DHDP monolayer. Here, we found that a low pH value of 2.5 is essential when stabilizing a DHDP monolayer on the surface of aqueous solutions containing Fe(III). The pH was adjusted with HCl.
- **2.6.** X-ray Instrumentation and Langmuir Trough Setup. A liquid surface scattering instrument located at beamline 15-ID, NSF's ChemMatCARS, of the Advanced Photon Source, Argonne National Laboratory, was used for the X-ray experiments. 40,41 X-ray energy was set to 10 keV. The Langmuir trough was inside a closed box purged with helium to reduce beam damage and air scattering. 42 The helium was bubbled through water prior to entering the trough box. Beam damage was avoided by collecting data in appropriate time intervals as indicated by previous tests. The sample was shifted horizontally to place the X-ray beam on a fresh spot on the sample between scans.
- 2.7. X-ray Fluorescence Near Total Reflection (XFNTR). XFNTR determines the surface density (number of ions per area) by measuring fluorescence spectra from samples for a series of wave vector transfers Q_{τ} near the critical $Q_{\rm c}$ for total reflection, where $Q_{\rm z}=2k_0\sin\alpha$, $k_0=2\pi/\lambda$ is the wave number and α is the incident angle. ⁴³ The X-ray fluorescence spectrum was recorded by a Vortex-60EX multicathode energy dispersive X-ray detector placed perpendicularly above the surface. The incident beam intensity and detector dead time corrections were used to normalize the fluorescence spectrum. After normalization, the Klpha fluorescence peak was fit to a Gaussian function to get its integrated area, which gives the XFNTR signal. The XFNTR signal is modeled by integrating the X-ray intensity and the metal-ion concentration over the overlap region between the detection volume and the X-ray path in the aqueous phase, as described previously.^{22,44} XFNTR was measured after the surface tension of aqueous solutions stabilized (as illustrated in Figure S3). For the DHDP monolayer experiments, XFNTR was measured after the surface pressure was stable for at least 10 min to ensure that the sample was in equilibrium. Calibration curves from reference samples are shown in Figure S4.
- **2.8. PMF Calculation.** Classical molecular dynamics simulations utilized Desmond software employing the Particle Mesh Ewald (PME) treatment.⁴⁵ The SPC/E water model was

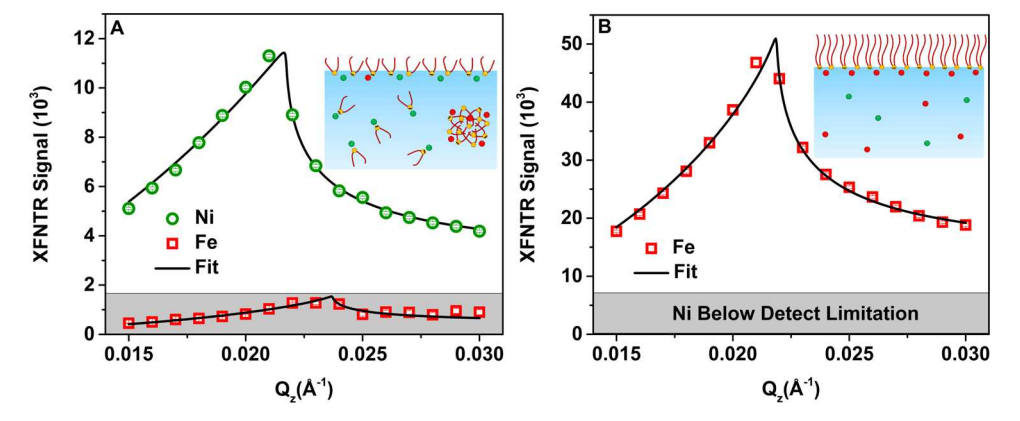


Figure 1. Integrated fluorescence intensity of Fe(III) and Ni(II) $K\alpha$ emission lines as a function of Q_a for samples containing a mixture of Fe(III) and Ni(II). (A) HDEHP-aqueous solution, pH 5.0 (20 μM HDEHP, 1.67 μM FeCl₃, 1.67 μM NiCl₂), (B) DHDP monolayer on pH 2.5 aqueous subphase (1.67 μM FeCl₃, 1.67 μM NiCl₂). Insets show schematic representations of the location of extractants and ions.

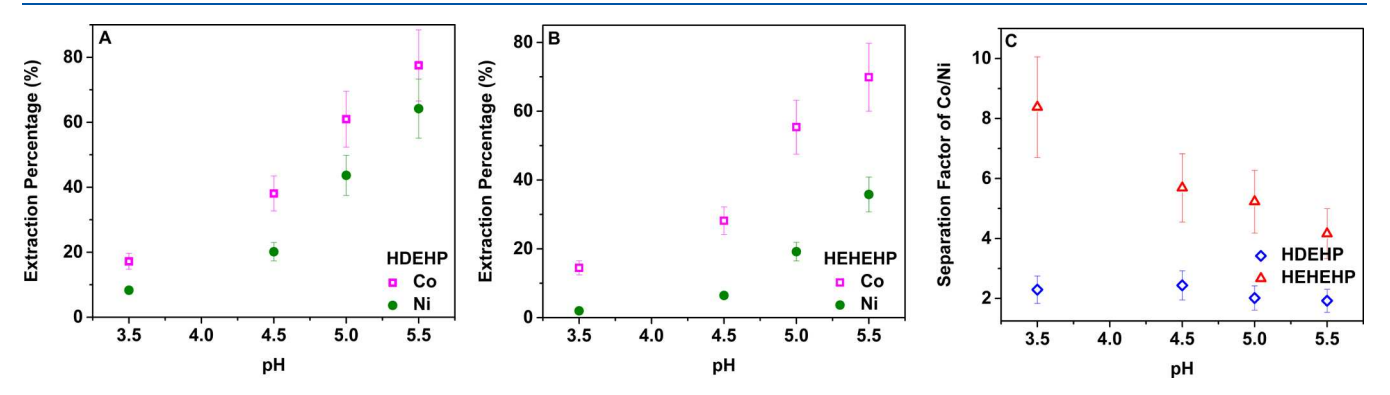


Figure 2. Liquid—liquid extraction behavior of Co(II) and Ni(II) in HDEHP and HEHEHP extraction systems as a function of pH. (A) Extraction percentage E defined in eq 1 for the aqueous-dodecane extraction system containing HDEHP. (B) Extraction percentage E for the aqueous-dodecane extraction system containing HEHEHP. (C) Separation factors β of Co(II)/Ni(II) at different pH. The concentration of extractants in the dodecane phase is 0.5 mM. The initial aqueous concentrations of Co(II) and Ni(II) are both 0.1 mM. The volume ratio of organic phase to aqueous phase is 1:1. Calculated uncertainties in the plots assume uncertainties of $\pm 10\%$ in the underlying ICP measurements.

used. Force field parameters were taken from Merz and coworkers who employed the thermodynamic integration method to design LJ parameters for 24 M(II) ions. ⁴⁶ The parameters were validated against measured ion—oxygen distances, as well as a comparison to van der Waals radii obtained using the quantum mechanical scaling principle (QMSP) method by Stokes.

These simulations were used to calculate the potential of mean force as a function of distance $d_{\rm MP}$ from the P atom of the DEHP⁻ and EHEHP⁻ to the metal ion by the WHAM method. The distance $d_{\rm MP}$ was restrained with a force constant of 250 kcal mol⁻¹ Å⁻². A step size of 0.025 Å was used when changing $d_{\rm MP}$ from 8 to 4.5 Å, and a step size of 0.01 Å was used when changing $d_{\rm MP}$ from 4.5 to 3 Å. Each step was run for 2 ns at a constant temperature of 300 K. The free energy was calculated from

$$A(d_{\rm MP}) = -k_{\rm B}T \ln P_{\rm ub}(d_{\rm MP}) \tag{4}$$

where $k_{\rm B}$ is the Boltzmann constant, T is the temperature of the simulation, and $P_{\rm ub}$ ($d_{\rm MP}$) is the unbiased distribution of metal—phosphorus distances.

3. RESULTS

3.1. Fe(III) and Ni(II) Adsorption. Before discussing the subtler distinction of interactions between Co(II) and Ni(II) with organophosphorous extractants we provide the example

of competitive binding of Fe(III) and Ni(II) to the surface of aqueous solutions in the presence of phosphoric acid extractants HDEHP and DHDP. A previous study of binding of Fe(III) to DHDP at the surface of aqueous solutions of FeCl₃ demonstrated strong adsorption that could be explained only by a combination of electrostatic interactions and covalent bonds. In this study the pH-dependent speciation of Fe(III) into Fe³⁺, Fe(OH)²⁺, and Fe(OH)₃ was shown to be important for the covalent aspect of the binding. The strong binding found in this study is consistent with the preferential extraction of Fe(III) over Ni(II) in solvent extraction processes that utilize organophosphorus extractants.

Figure 1A shows the result of XFNTR measurements from the surface of aqueous solutions of water-soluble HDEHP and a mixture of FeCl₃ and NiCl₂ (20 μ M HDEHP, 1.67 μ M FeCl₃, 1.67 μ M NiCl₂). These measurements probe the presence of specific ions within roughly 5 to 10 nm of the surface; however, the contribution of ions that are not bound to surface adsorbed extractants is expected to be negligible because of the low bulk concentrations used in these experiments. Figure 1A shows clearly that the predominant ion at the surface is Ni(II). Since neither ion would be strongly adsorbed to this surface in the absence of HDEHP, the Ni(II) ions at the surface must be complexed to HDEHP at the surface. The lines in Figure 1A are fits to the data which yield a surface density of 3.7×10^{-3} ions per Å² (or 270 Å² per ion)

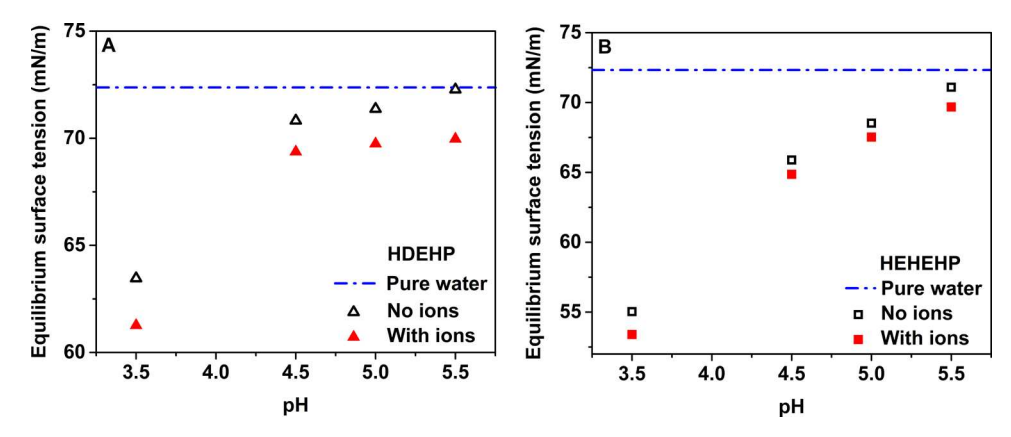


Figure 3. Equilibrium surface tension measurements at the aqueous–vapor interface of aqueous solutions containing either HDEHP (20 μ M) or HEHEHP (22.5 μ M) with and without a mixture of Co(II) and Ni(II) ions (HDEHP: 1.11 μ M for each ion, HEHEHP: 1.25 μ M for each ion). (A, B) Equilibrium surface tensions as a function of pH. See Table S1 for values and Figure S3 for the underlying time-dependent measurements.

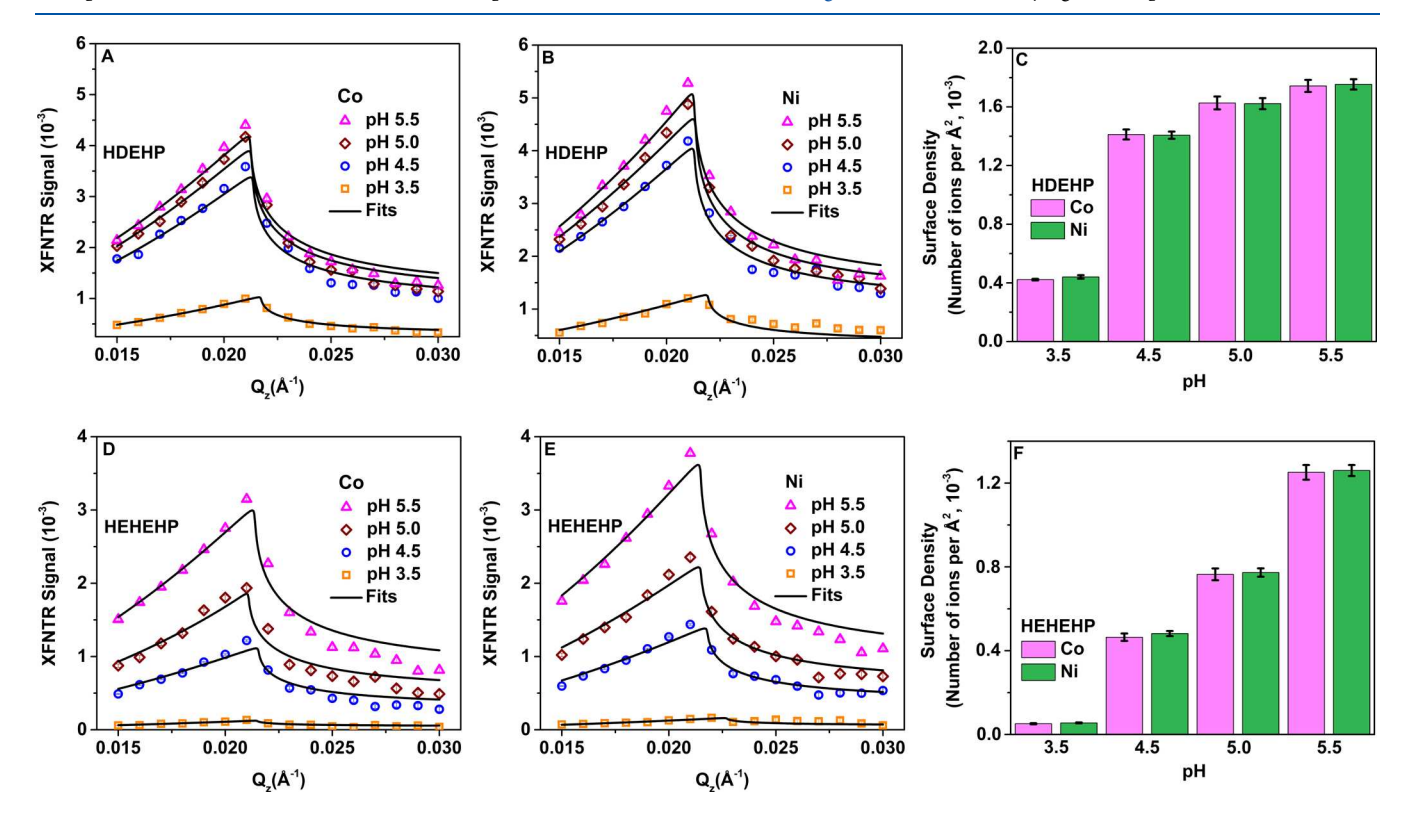


Figure 4. XFNTR measurements from the liquid–vapor interface of equilibrated aqueous samples of the same composition and pH as shown in Figure 3. The symbols in (A), (B), (D), and (E) show the integrated fluorescence intensity of Co(II) and Ni(II) Kα emission lines as a function of Q_z measured from samples containing extractants (HDEHP (20 μM) or HEHEHP (22.5 μM)) and a mixture of Co(II) (1.11 μM for HDEHP and 1.25 for HEHEHP) at different pHs. (A) Co(II) XFNTR from HDEHP solutions, (B) Ni(II) XFNTR from HDEHP solutions, (C) surface densities of Co(II) and Ni(II) in HDEHP solutions, (D) Co(II) XFNTR from HEHEHP solutions, (E) Ni(II) XFNTR from HEHEHP solutions, and (F) surface densities of Co(II) and Ni(II) in HEHEHP solutions.

for Ni(II) compared to 8.6×10^{-4} ions per Å² (or 1164 Å² per ion) for Fe(III), which demonstrates the much lower surface density of Fe(III).

Figure 1B shows the effect of confining the extractants to the water surface. This is accomplished by spreading a monolayer of the insoluble extractant DHDP onto the surface. The surface pressure is maintained at 10 mN/m to form a close-packed monolayer of DHDP. The phosphoric acid headgroups of the two extractants, HDEHP and DHDP are the same, yet the ions bound to the surface are very different. When a monolayer of DHDP is present, Fe(III) dominates the surface with a surface density of 2.8×10^{-2} ions per Å² (or 36 Å² per ion)

compared to a surface density of Ni(II) that is below our detection limit, which we estimate as roughly 2×10^{-5} ions per Å² (or 50,000 Å² per ion).

These measurements illustrate that the ion which is expected to be more strongly bound to a phosphoric acid headgroup, in this case Fe(III), is found predominantly at the water surface when phosphoric acid extractants are confined to the surface, but not when the extractants are soluble in the bulk phase. Before making a direct comparison with XFNTR measurements that distinguish Ni(II) and Co(II) we describe a series of measurements in the next two sections that characterize the

solution behavior of Ni(II) and Co(II) with two soluble extractants, HDEHP and HEHEHP.

3.2. Extraction Selectivity of Co(II) and Ni(II) in a Conventional Solvent Extraction Process. As described in Section 2.3, the extraction percentage E (eq 1) was measured by placing organic and aqueous solutions in contact, mixing them, and analyzing the initial and final concentrations in the aqueous phase with ICP-OES. Figure 2 shows the effect of pH on the extraction percentage E of mixtures of Co(II) and Ni(II) in solvent extraction systems containing either HDEHP or HEHEHP. Preferential extraction of Co(II) is observed in both extraction systems and the extraction percentage of Co(II) and Ni(II) increases with pH for both extraction systems. Figure 2C shows that the separation factor, β , of Co(II) to Ni(II) with HEHEHP is higher than with HDEHP, indicating that HEHEHP is better at selecting Co(II) from Ni(II) than HDEHP. These results are consistent with the published literature. 9,11,12

3.3. Surface Tension of Aqueous Solutions of Extractants and Co(II)/Ni(II) Mixtures. Both HDEHP and HEHEHP are slightly soluble in water. Figure 3 shows the surface tension of aqueous solutions of HDEHP and HEHEHP which contain mixtures of Co(II) and Ni(II) at different pH. The equilibrium surface tension shown in Figure 3A,B of HDEHP-aqueous solution and HEHEHP-aqueous solutions increases with pH, suggesting larger adsorption for lower values of pH. The effect of pH on the surface tension can be attributed to the deprotonation/protonation equilibrium of HDEHP and HEHEHP. Protonated extractants have a higher surface affinity than the deprotonated versions (DEHP- and EHEHP⁻). Since the protonated species is more prevalent at lower pH, the surface tension is lower at lower pH. In addition, the surface tension values change only slightly over the range of pH from 4.5 to 5.5 for HDEHP but they rise more rapidly over this range for HEHEHP (Figure 3A,B). This can be explained by the different pKa values of HDEHP (p $K_a = 3.24$) and HEHEHP (p $K_a = 4.57$). Most HDEHP will be deprotonated for pH values above 4.5 (Figure S2A), while the ratio of deprotonated EHEHP- to HEHEHP continues to increase as the pH rises above 4.5 (Figure S2B).

Figure 3 also shows that the metal-ion-induced reduction in surface tension of HDEHP-aqueous solution is larger than for HEHEHP-aqueous solutions. As we have demonstrated in previous work, the surface tension of HDEHP-aqueous solutions will decrease when ions are added into the solution due to the adsorption of ion—extractant complexes.³⁴ Therefore, the adsorption of ion-HDEHP complexes to the surface is likely larger than that of ion-HEHEHP complexes. In the next section, X-ray measurements are used to clarify the interfacial nature of these systems.

3.4. XFNTR from HDEHP- and HEHEHP-Aqueous Solutions Containing Co(II) and Ni(II). XFNTR is an interface selective technique with element sensitivity. It probes the presence and surface density of metal ions at the interface. Figure 4 shows XFNTR data from the liquid–vapor interface of HDEHP and HEHEHP-aqueous solutions containing a mixture of Co(II) and Ni(II) at different pH. Figure 4C,F and Table 1 show that the surface density of Co(II) and Ni(II) on both HDEHP and HEHEHP solutions increases with pH, though the values are generally larger for HDEHP solutions.

Figure 4 shows that the ion surface density of HDEHP solutions exhibits a large increase when the pH is increased

Table 1. Surface Area Per Ion (Å²) of Co and Ni at the Aqueous-Vapor Interface of Solutions Containing Co, Ni, HDEHP, and HEHEHP Determined by the XFNTR Measurements Shown in Figure 4

	HDEHP		НЕНЕНР	
pН	Со	Ni	Со	Ni
3.5	2370 ± 30	2270 ± 60	19500 ± 1000	18100 ± 700
4.5	710 ± 20	710 ± 10	2150 ± 90	2080 ± 60
5.0	610 ± 20	620 ± 10	1310 ± 50	1290 ± 30
5.5	570 ± 10	570 ± 10	800 ± 20	790 ± 20

from 3.5 to 4.5 but smaller increases with further increase of pH. In contrast, the ion surface densities on HEHEHP solutions exhibit a nearly steady increase with pH. Note that these trends cannot be deduced from our surface tension measurements in Figure 3 which were not designed to measure the adsorption of ions. The surface tension is reduced primarily as a result of extractant adsorption, whereas XFNTR measures the surface density of ions. The results in Figures 3 and 4 suggest that increasing pH reduces the adsorption of extractants at the water surface while increasing the adsorption of Co(II) and Ni(II). This is a consequence of the greater deprotonation of extractants at a high pH which then have weaker surface affinity but stronger affinity to Co(II) and Ni(II). Notably, the surface densities of Co(II) and Ni(II) for a given extractant are very similar at each value of pH. This unexpected result shows that the surface adsorption selectivity of Co(II) and Ni(II) is very low when the only source of extractant is soluble HDEHP and HEHEHP in water.

3.5. XFNTR from Co(II) and Ni(II) Bound to DHDP Monolayers. For comparison, the adsorption of Co(II) and Ni(II) to a phosphoric acid extractant that is confined to the surface as a monolayer was measured. Dihexadecyl phosphate (DHDP) has the same headgroup as HDEHP but cannot dissolve into the bulk water because of its longer hydrocarbon chain. Here, it is studied as a monolayer at the water—vapor interface of aqueous solution mixtures of Ni(II) and Co(II). In contrast, Figures 4C and 5C show that the surface density of Co(II) on a DHDP monolayer is substantially higher at all values of pH than the surface density of Ni(II). This trend is consistent with the preferential extraction of Co(II) over Ni(II) in solvent extraction that uses phosphoric acid extractants (Table 2).

3.6. Potentials of Mean Force from Molecular Dynamics Simulations. Potentials of mean force (PMF) between a single deprotonated extractant and a single ion (Ni(II) or Co(II)) in bulk water were simulated with classical molecular dynamics (Figure 6). The differences in the PMF (or free energy profile) reveal the stronger interaction between the deprotonated extractants and Co(II) than with Ni(II).

4. DISCUSSION

The role of extractant solubility in the aqueous phase was explored in this work for transition-metal ions Co(II) and Ni(II). In some sense, this work is a follow-up to recent studies of lanthanide extraction, which demonstrated that bulk solubility may play an antagonistic role in the preferential extraction of heavy over light lanthanides by HDEHP. ³⁴ In that work, a light lanthanide, Nd, and a heavy lanthanide, Er, were investigated. It is known that the separation factor can reach about 100 for these two elements, greatly favoring the extraction of Er in solvent extraction processes with

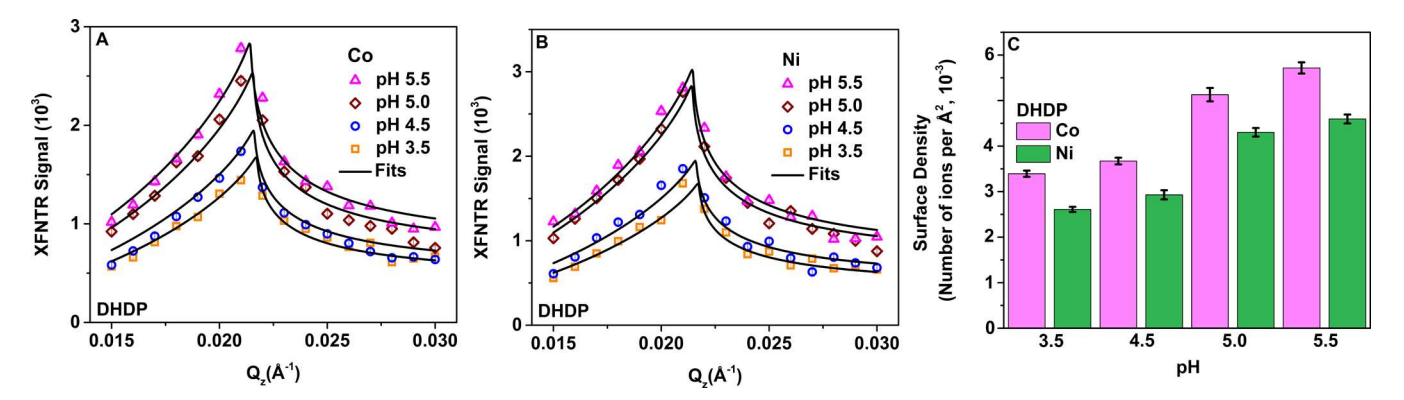


Figure 5. XFNTR from the liquid-vapor interface of aqueous solutions of a mixture of Co(II) (10 μ M) and Ni(II) (10 μ M) ions that contain a monolayer of DHDP at a surface pressure of 10 mN/m. (A, B) Integrated fluorescence intensity of Co(II) and Ni(II) K α emission lines as a function of Q_x . (C) Surface density of Co(II) and Ni(II) at different pH.

Table 2. Surface Area Per Ion (\mathring{A}^2) of Co and Ni at the DHDP Monolayer Determined by the XFNTR Measurements Shown in Figure 5

pН	Со	Ni
3.5	295 ± 6	383 ± 8
4.5	272 ± 6	340 ± 10
5.0	195 ± 6	232 ± 5
5.5	175 ± 4	218 ± 5

HDEHP.⁵¹ Also like the current work, phosphoric acid extractants HDEHP and DHDP were used; both have the same phosphoric acid headgroup that interacts with the metal ions. XFNTR measurements from the surface of aqueous solutions of soluble HDEHP and a mixture of the trivalent lanthanides Nd(III) and Er(III) demonstrated that Nd(III) is overwhelmingly preferred at the surface, in opposition to our expectation that Er(III) would be found at the surface because it is much more likely to be extracted in a liquid-liquid solvent extraction process. However, XFNTR measurements from the surface of aqueous solutions of a mixture of Nd(III) and Er(III) in the presence of a DHDP monolayer at the surface showed that Er(III) is greatly preferred at the surface. Therefore, the element that is preferentially extracted in solvent extraction is found preferentially at the surface of an aqueous solution only when the extractant is confined to the surface. In spite of the stronger attraction of Er(III) for the

phosphoric acid headgroup, it did not go to the surface when in competition with Nd(III) for HDEHP. Instead, it likely formed an ion—extractant complex that preferred the bulk aqueous phase. These published measurements suggested that complexation of these metal ions with a soluble extractant in the bulk aqueous phase would act to hinder the intended extraction of the heavier lanthanide Er(III), whereas complexation with an extractant at the surface would favor it.

To extend this work to investigate the separation of Co(II) and Ni(II), we first compared Fe(III) to Ni(II) because of the anticipated much greater affinity of Fe(III) to the extractants. Previous studies have demonstrated preferential extraction of Fe(III) over Ni(II) in solvent extraction processes utilizing HDEHP, as well as strong binding of Fe(III) to DHDP. ^{36,49} Like the lanthanide measurements, XFNTR measurements in Figure 1 demonstrated that Ni ions were found predominantly at the surface when soluble HDEHP was used, but Fe ions occupied the surface when the insoluble DHDP was confined to a monolayer at the surface. Once again, it is surprising that the much stronger interaction of Fe(III) over Ni(II) for HDEHP or DHDP did not just lead to preferential interactions with the extractants wherever they were, that is, either in the bulk or at the surface. Instead, it appears that the complexation of Fe(III) with HDEHP in bulk water is so strongly favored that it leaves the surface available for occupation by Ni(II)-HDEHP complexes. Here, we see the results of competing

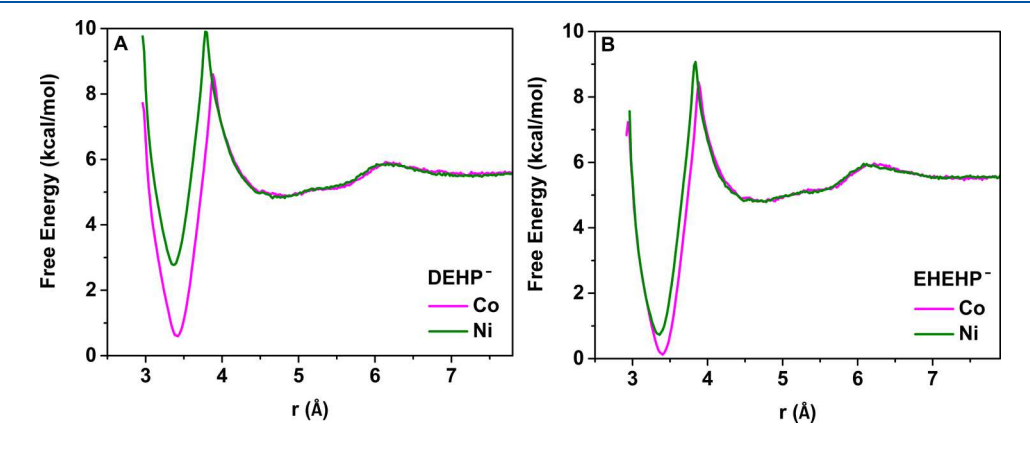


Figure 6. MD simulations of the potential of mean force (PMF or free energy profile) between a single ion (Co(II) or Ni(II)) and a single deprotonated extractant in bulk water. (A) DEHP $^-$. (B) EHEHP $^-$. The deeper minimum for Co(II) for both the DEHP $^-$ and EHEHP $^-$ reveals a stronger interaction with Co(II) than with Ni(II).

equilibrium between ion—extractant complexes soluble in the bulk and at the surface for two different ions. This is a complex equilibrium that depends not only on the different interactions between HDEHP and the two different ions but also on the different structures of bulk and surface complexes. Previously published molecular dynamics (MD) simulations showed that lanthanide-HDEHP complexes soluble in bulk water are micelles containing many ions and extractants, but surface complexes are expected to contain a single ion surrounded by a few extractants.³⁴

In this work, we added HEHEHP to the selection of extractants that was studied because it is known that the phosphonic acid HEHEHP has a higher selectivity than HDEHP for extracting Co(II) over Ni(II). HEHEHP is preferred in industrial processes to separate these two elements. This was illustrated in the solvent extraction measurements shown in Figure 2, which showed that although the percentages of extraction E of both Co(II) and Ni(II) are slightly higher for HDEHP than for HEHEHP, the selectivity of Co(II) over Ni(II) is much higher for HEHEHP as indicated by the larger separation factors β for a range of pH. Note that in comparison to the value of β of roughly 100 that is relevant to the previous studies of Er(III) and Nd(III), even the higher values of β measured for HEHEHP are relatively small.

XFNTR measurements of aqueous solutions of mixtures of Co(II) and Ni(II) with either HDEHP or HEHEHP revealed that the ion density was larger at the surface of HDEHP solutions than at the surface of HEHEHP solutions for all values of pH studied (Figure 4). This is consistent with the greater reduction in surface tension of HDEHP-aqueous solutions upon addition of metal ions than the reduction observed in HEHEHP-aqueous solutions since both techniques show that the presence of metal ions has a greater effect on the surface in the presence of HDEHP (Figure 3). This may also be related to the greater percentages of extraction E by HDEHP than by HEHEHP since more ions would need to pass through a liquid—liquid interface to increase E; however, more investigation is needed to prove this connection.

Interestingly, although the surface densities of ions vary by more than a factor of 10 under the conditions shown in Figure 4, the surface density at each pH for each soluble extractant is essentially the same for Co(II) and Ni(II). Here, we define a surface selectivity parameter for Co(II) and Ni(II) as the surface density of Co(II) divided by the surface density of Ni(II). Surface selectivity values greater than 1, for example, reveal a preferential adsorption of Co(II) to the surface. Figure 7 shows that all values of surface selectivity for HDEHP and HEHEHP are 1 within experimental uncertainty for the measured values of pH. Our observation of a surface selectivity of 1 represents a suppression of a larger surface selectivity that we might have expected based upon the known preferential extraction of Co over Ni, as well as the stronger interaction of Co(II) with extractants demonstrated by the simulated potentials of mean force. However, if our previous studies of lanthanides and the Fe/Ni system are a guide, then we should have measured a surface selectivity of less than 1 for HDEHP and DHDP. The fact that the surface selectivity is essentially one may be the result of the smaller differences between the competing ions Co and Ni than the differences between either Nd and Er (separation factor of around 100) or between Fe and Ni (separation factor of more than 1000).

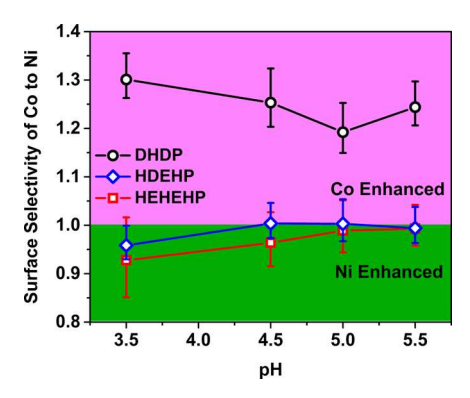


Figure 7. Surface selectivity of Co(II) to Ni(II) for different extractants and values of pH.

Also shown in Figure 7 is the preferential surface selectivity for Co(II) when a monolayer of DHDP is confined to the water surface. Here, we observe that the ion that interacts more strongly with the extractant headgroup, which in these cases is also the ion that is preferentially extracted in liquid—liquid solvent extraction, is found preferentially at the surface when the extractant is confined to the surface. Note, however, that in this case the preference for Co(II) is slight, just on the order of 30%, whereas similar behavior measured for the Fe/Ni system and previously observed in the Er/Nd system exhibited an overwhelming preference for the ion that is also extracted in solvent extraction. 34

5. CONCLUSIONS

Measurements of the surface of aqueous solutions containing water-soluble extractants HDEHP or HEHEHP and a mixture of Co(II) and Ni(II) ions reveal comparable adsorption behaviors of Co(II) and Ni(II) for a solution pH of 3.5, 4.5, 5.0, and 5.5. Surface tension measurements show a greater reduction in the surface tension in the HDEHP-aqueous solution upon inclusion of metal ions than when metal ions are included in the HEHEHP-aqueous solution. XFNTR results demonstrate that the surface adsorption of Co(II) is similar to that of Ni(II) in both HDEHP and HEHEHP-aqueous solutions for all values of pH investigated. However, preferential adsorption of Co(II) is found at the solution surface when a water-insoluble DHDP monolayer is present. The latter is consistent with our expectation that more Co(II) than Ni(II) should be found at the surface because conventional solvent extraction processes favor extraction of Co(II) with these extractants. However, the reduction in the selectivity between Co(II) and Ni(II) when extractants are soluble in water may result from the stronger affinity of Co(II) to the aggregates that form in the aqueous solution. This would be consistent with the preferential attraction of Co(II) over Ni(II) to DEHP- that was demonstrated by our MD simulations of the potential of mean force shown in Figure 6.

Studies of the adsorption behavior of Fe(III) and Ni(II) with water-soluble extractants demonstrate a reduction in selectivity to the point of reversing it so that Ni(II) is primarily adsorbed to the surface. This is similar to previous observations of the adsorption behavior of Er(III) and Nd(III) with water-soluble extractant HDEHP. In all three cases—Co/Ni, Fe/Ni, and Er/Nd—the element that is preferentially extracted is also found preferentially at the surface when the extractant is confined to the surface, as observed with the water-insoluble extractant DHDP. These results suggest that

metal ions with stronger affinity to water-soluble extractants will be held back in the aqueous solution. The present work emphasizes the antagonistic role of complexation within aqueous solution in the solvent extraction of Co/Ni and suggests the advantage of metal-ion complexation at the interface for solvent extraction. Ongoing experiments at the liquid—liquid interface are exploring the suggested antagonistic role of aqueous complexation in liquid—liquid extraction processes.

ASSOCIATED CONTENT

Supporting Information

The Supporting Information is available free of charge at https://pubs.acs.org/doi/10.1021/acs.jpcb.2c08412.

Fe-Cl and Co-Cl species in aqueous solution as a function of Cl- concentration; pH dependence of ratio of the protonated and deprotonated form of extractant (HDEHP and HEHEHP) in the aqueous solution; surface tension (including time-dependent data and equilibrium values); and XFNTR of calibration measurements (PDF)

AUTHOR INFORMATION

Corresponding Authors

Wei Bu — NSF's ChemMatCARS, Pritzker School of Molecular Engineering, University of Chicago, Chicago, Illinois 60637, United States; oorcid.org/0000-0002-9996-3733; Email: bu@cars.uchicago.edu

Mark L. Schlossman — Department of Physics, University of Illinois at Chicago, Chicago, Illinois 60607, United States; orcid.org/0000-0003-3238-1250; Email: schloss@uic.edu

Authors

Pan Sun — Department of Physics, University of Illinois at Chicago, Chicago, Illinois 60607, United States; NSF's ChemMatCARS, Pritzker School of Molecular Engineering, University of Chicago, Chicago, Illinois 60637, United States; orcid.org/0000-0002-6128-8656

Erik A. Binter – Department of Physics, University of Illinois at Chicago, Chicago, Illinois 60607, United States

Trung Vo – Department of Physics, University of Illinois at Chicago, Chicago, Illinois 60607, United States

Ilan Benjamin – Department of Chemistry and Biochemistry, University of California, Santa Cruz, California 95064, United States; ocid.org/0000-0003-0056-4925

Mrinal K. Bera — NSF's ChemMatCARS, Pritzker School of Molecular Engineering, University of Chicago, Chicago, Illinois 60637, United States; orcid.org/0000-0003-0698-5253

Binhua Lin — NSF's ChemMatCARS, Pritzker School of Molecular Engineering, University of Chicago, Chicago, Illinois 60637, United States; orcid.org/0000-0001-5932-4905

Complete contact information is available at: https://pubs.acs.org/10.1021/acs.jpcb.2c08412

Author Contributions

The manuscript was written through contributions of all authors. All authors have given approval to the final version of the manuscript.

Notes

The authors declare no competing financial interest.

ACKNOWLEDGMENTS

This research is performed using funding received from the U.S. Department of Energy, Office of Science, Office of Basic Energy Sciences Separations Program under Award Number DE-SC0018200 to M.L.S. and I.B. Partial support for T.V. and E.B. came from the DOE Office of Nuclear Energy's Nuclear Energy University Program under Award Number DE-NE0008779 to M.L.S. NSF's ChemMatCARS Sector 15 is funded by the Divisions of Chemistry (CHE) and Materials Research (DMR), National Science Foundation, under grant number NSF/CHE-1834750. The authors thank Artem V. Gelis (UNLV) for purifying HDEHP and HEHEHP. They also thank Xiao-Min Lin for measuring the concentration of metal ions in the aqueous solution by ICP-OES measurements performed at the Center for Nanoscale Materials, Argonne National Laboratory. Use of the Advanced Photon Source, the Center for Nanoscale Materials and an Office of Science User Facility operated for the U.S. Department of Energy (DOE) Office of Science by Argonne National Laboratory, was supported by the U.S. DOE under Contract No. DE-AC02-06CH11357.

ABBREVIATIONS

HDEHP, bis(2-ethylhexyl) phosphoric acid; HEHEHP, 2-ethylhexylphosphonic acid mono-2-ethylhexyl ester; DHDP, dihexadecyl phosphoric acid; XFNTR, X-ray fluorescence near total reflection

REFERENCES

- (1) Fu, X. K.; Beatty, D. N.; Gaustad, G. G.; Ceder, G.; Roth, R.; Kirchain, R. E.; Bustamante, M.; Babbitt, C.; Olivetti, E. A. Perspectives on Cobalt Supply through 2030 in the Face of Changing Demand. *Environ. Sci. Technol.* **2020**, *54*, 2985–2993.
- (2) Heijlen, W.; Franceschi, G.; Duhayon, C.; Van Nijen, K. Assessing the adequacy of the global land-based mine development pipeline in the light of future high-demand scenarios: The case of the battery-metals nickel (Ni) and cobalt (Co). *Resour. Policy* **2021**, 73, No. 102202.
- (3) Alvial-Hein, G.; Mahandra, H.; Ghahreman, A. Separation and recovery of cobalt and nickel from end of life products via solvent extraction technique: A review. *J. Cleaner Prod.* **2021**, 297, No. 126592
- (4) Chen, L.; Tang, X.; Zhang, Y.; Li, L.; Zeng, Z.; Zhang, Y. Process for the recovery of cobalt oxalate from spent lithium-ion batteries. *Hydrometallurgy* **2011**, *108*, 80–86.
- (5) Yuan, L.; Wen, J.; Ning, P.; Yang, H.; Sun, Z.; Cao, H. Inhibition Role of Solvation on the Selective Extraction of Co(II): Toward Eco-Friendly Separation of Ni and Co. ACS Sustainable Chem. Eng. 2022, 10, 1160–1171.
- (6) Nayl, A. A. Extraction and separation of Co(II) and Ni(II) from acidic sulfate solutions using Aliquat 336. *J. Hazard. Mater.* **2010**, 173, 223–230.
- (7) Okatan, A.; Eyüpoğlu, V.; Kumbasar, R. A.; Turgut, H. İ. In Synergistic extraction and separation of Co(II)/Ni(II) by solvent extraction technique using TIOA/TOPO as carriers, AIP Conference Proceedings; AIP Publishing LLC, 2016; p 020111.
- (8) Liang, Z.; Bu, W.; Schweighofer, K. J.; Walwark, D. J.; Harvey, J. S.; Hanlon, G. R.; Amoanu, D.; Erol, C.; Benjamin, I.; Schlossman, M. L. Nanoscale view of assisted ion transport across the liquid—liquid interface. *Proc. Natl. Acad. Sci. U.S.A.* **2019**, *116*, 18227—18232.
- (9) Hachemaoui, A.; Belhamel, K.; Bart, H.-J. Emulsion liquid membrane extraction of Ni(II) and Co(II) from acidic chloride

- solutions using bis-(2-ethylhexyl) phosphoric acid as extractant. *J. Coord. Chem.* **2010**, *63*, 2337–2348.
- (10) Kasaini, H.; Nakashio, F.; Goto, M. Application of emulsion liquid membranes to recover cobalt ions from a dual-component sulphate solution containing nickel ions. *J. Membr. Sci.* **1998**, *146*, 159–168.
- (11) Parhi, P. K.; Panigrahi, S.; Sarangi, K.; Nathsarma, K. C. Separation of cobalt and nickel from ammoniacal sulphate solution using Cyanex 272. *Sep. Purif. Technol.* **2008**, *59*, 310–317.
- (12) Tait, B. K. Cobalt-nickel separation: the extraction of cobalt(II) and nickel(II) by Cyanex 301, Cyanex 302 and Cyanex 272. *Hydrometallurgy* **1993**, 32, 365–372.
- (13) Gras, M.; Papaiconomou, N.; Schaeffer, N.; Chainet, E.; Tedjar, F.; Coutinho, J. A. P.; Billard, I. Ionic-Liquid-Based Acidic Aqueous Biphasic Systems for Simultaneous Leaching and Extraction of Metallic Ions. *Angew. Chem., Int. Ed.* **2018**, *57*, 1563–1566.
- (14) Preston, J. S. Solvent Extraction of Cobalt(ll) and Nickel(ll) by a Quaternary Ammonium Thiocyanate. *Sep. Sci. Technol.* **1982**, *17*, 1697–1718.
- (15) Cheng, C. Y.; Boddy, G.; Zhang, W.; Godfrey, M.; Robinson, D. J.; Pranolo, Y.; Zhu, Z.; Wang, W. Recovery of nickel and cobalt from laterite leach solutions using direct solvent extraction: Part 1 selection of a synergistic SX system. *Hydrometallurgy* **2010**, *104*, 45–52.
- (16) Cheng, C. Y.; Boddy, G.; Zhang, W.; Godfrey, M.; Robinson, D. J.; Pranolo, Y.; Zhu, Z.; Zeng, L.; Wang, W. Recovery of nickel and cobalt from laterite leach solutions using direct solvent extraction. *Hydrometallurgy* **2010**, *104*, 53–60.
- (17) Hughes, M. A.; Rod, V. A general model to account for the liquid/liquid kinetics of extraction of metals by organic acids. *Faraday Discuss. Chem. Soc.* **1984**, *77*, 75–84.
- (18) Testard, F.; Berthon, L.; Zemb, T. Liquid-liquid extraction: An adsorption isotherm at divided interface? *C. R. Chim.* **2007**, *10*, 1034–1041.
- (19) Watarai, H.; Freiser, H. Role of the Interface in the Extraction Kinetics of Zinc and Nickel Ions with Alkyl-Substituted Dithizones. *J. Am. Chem. Soc.* **1983**, *105*, 189–190.
- (20) Chowdhury, A. U.; Lin, L.; Doughty, B. Hydrogen-Bond-Driven Chemical Separations: Elucidating the Interfacial Steps of Self-Assembly in Solvent Extraction. *ACS Appl. Mater. Interfaces* **2020**, *12*, 32119–32130.
- (21) Nayak, S.; Lovering, K.; Bu, W.; Uysal, A. Anions Enhance Rare Earth Adsorption at Negatively Charged Surfaces. *J. Phys. Chem. Lett.* **2020**, *11*, 4436–4442.
- (22) Bu, W.; Yu, H.; Luo, G. M.; Bera, M. K.; Hou, B. Y.; Schuman, A. W.; Lin, B. H.; Meron, M.; Kuzmenko, I.; Antonio, M. R.; Soderholm, L.; Schlossman, M. L. Observation of a Rare Earth Ion-Extractant Complex Arrested at the Oil Water Interface During Solvent Extraction. *J. Phys. Chem. B* **2014**, *118*, 10662–10674.
- (23) Scoppola, E.; Watkins, E.; Li Destri, G.; Porcar, L.; Campbell, R. A.; Konovalov, O.; Fragneto, G.; Diat, O. Structure of a liquid/liquid interface during solvent extraction combining X-ray and neutron reflectivity measurements. *Phys. Chem. Chem. Phys.* **2015**, 17, 15093–15097.
- (24) Scoppola, E.; Watkins, E. B.; Campbell, R. A.; Konovalov, O.; Girard, L.; Dufreche, J. F.; Ferru, G.; Fragneto, G.; Diat, O. Solvent Extraction: Structure of the Liquid-Liquid Interface Containing a Diamide Ligand. *Angew. Chem., Int. Ed.* **2016**, *55*, 9326–9330.
- (25) Bu, W.; Flores, K.; Pleasants, J.; Vaknin, D. Preferential Affinity of Calcium Ions to Charged Phosphatidic Acid Surface from a Mixed Calcium/Barium Solution: X-ray Reflectivity and Fluorescence Studies. *Langmuir* **2009**, *25*, 1068–1073.
- (26) Uysal, A.; Rock, W.; Qiao, B.; Bu, W.; Lin, B. Two-Step Adsorption of PtCl₆²⁻ Complexes at a Charged Langmuir Monolayer: Role of Hydration and Ion Correlations. *J. Phys. Chem. C* **2017**, *121*, 25377–25383.
- (27) Kusaka, R.; Watanabe, M. The structure of a lanthanide complex at an extractant/water interface studied using heterodyne-

- detected vibrational sum frequency generation. Phys. Chem. Chem. Phys. 2018, 20, 2809-2813.
- (28) Kusaka, R.; Watanabe, M. Stoichiometry of Lanthanide-Phosphate Complexes at the Water Surface Studied Using Vibrational Sum Frequency Generation Spectroscopy and DFT Calculations. *J. Phys. Chem. B* **2021**, *125*, 6727–6731.
- (29) Yoo, S.; Qiao, B.; Douglas, T.; Bu, W.; Olvera de la Cruz, M.; Dutta, P. Specific Ion Effects in Lanthanide-Amphiphile Structures at the Air-Water Interface and Their Implications for Selective Separation. ACS Appl. Mater. Interfaces 2022, 14, 7504—7512.
- (30) Su, W.; Chen, J.; Jing, Y. Aqueous Partition Mechanism of Organophosphorus Extractants in Rare Earths Extraction. *Ind. Eng. Chem. Res.* **2016**, *55*, 8424–8431.
- (31) Principe, F.; Demopoulos, G. T. The solubility and stability of organophosphoric acid extractants in H2SO4 and HCl media. *Hydrometallurgy* **2003**, *68*, 115–124.
- (32) Belaïd, S.; Chachaty, C. NMR and ESR evidence of molecular aggregates in sodium dibutyl phosphate aqueous solutions. *J. Colloid Interface Sci.* **1982**, *86*, 277–281.
- (33) Wang, D.; Li, Y.; Wu, J.; Xu, G. Mechanism of the extractant loss in lanthanide extraction process with saponified organophosphorus acid extraction systems-II: formation of aqueous aggregates. Solv. Extr. Ion Exch. 1996, 14, 585–601.
- (34) Sun, P.; Binter, E. A.; Liang, Z.; Brown, M. A.; Gelis, A. V.; Benjamin, I.; Bera, M. K.; Lin, B.; Bu, W.; Schlossman, M. L. Antagonistic Role of Aqueous Complexation in the Solvent Extraction and Separation of Rare Earth Ions. *ACS Cent. Sci.* **2021**, *7*, 1908–1918
- (35) Nilsson, M.; Nash, K. L. A Review of the Development and Operational Characteristics of the TALSPEAK Process. *Solvent Extr. Ion. Exc.* **2007**, *25*, 665–701.
- (36) Sole, K. C. Solvent Extraction in the Hydrometallurgical Processing and Purification of Metals: Process Design and Selected Applications. In *Solvent Extraction and Liquid Membranes: Fundamentals and Applications in New Materials*; Aguilar, M.; Cortina, J. L., Eds.; Taylor & Francis, CRC Press: Boca Raton, 2008; pp 159–160.
- (37) Komasawa, I. O.; Otake, T.; Hattori, I. Separation of cobalt and nickel using solvent extraction with acidic organophosphorus compounds. *J. Chem. Eng. Japan* **1983**, *16*, 384–388.
- (38) Hu, Z. H.; Pan, Y.; Ma, W. W.; Fu, X. Purification of Organophosphorus Acid Extractants. *Solvent Extr. Ion Exc.* **1995**, *13*, 965–976.
- (39) Nayak, S.; Kumal, R. R.; Uysal, A. Spontaneous and Ion-Specific Formation of Inverted Bilayers at Air/Aqueous Interface. *Langmuir* **2022**, 38, 5617–5625.
- (40) Lin, B. H.; Meron, M.; Gebhardt, J.; Graber, T.; Schlossman, M. L.; Viccaro, P. J. The liquid surface/interface spectrometer at ChemMatCARS synchrotron facility at the Advanced Photon Source. *Phys. B* **2003**, 336, 75–80.
- (41) Pershan, P. S.; Schlossman, M. L. Liquid Surfaces and Interfaces: Synchrotron X-ray Methods; Cambridge University Press: Cambridge, 2012.
- (42) Sun, P.; Nowack, L. M.; Bu, W.; Bera, M. K.; Griesemer, S.; Reik, M.; Portner, J.; Rice, S. A.; Schlossman, M. L.; Lin, B. H. Free Thiols Regulate the Interactions and Self-Assembly of Thiol-Passivated Metal Nanoparticles. *Nano Lett.* **2021**, *21*, 1613–1619.
- (43) Bu, W.; Vaknin, D. X-ray fluorescence spectroscopy from ions at charged vapor/water interfaces. J. Appl. Phys. 2009, 105, No. 084911.
- (44) Bu, W.; Hou, B. Y.; Mihaylov, M.; Kuzmenko, I.; Lin, B. H.; Meron, M.; Soderholm, L.; Luo, G. M.; Schlossman, M. L. X-ray fluorescence from a model liquid/liquid solvent extraction system. *J. Appl. Phys.* **2011**, *110*, No. 102214.
- (45) Schrödinger Release 2017-2: Desmond Molecular Dynamics System, Maestro-Desmond Interoperability Tools, Schrödinger, New York, NY, 2017; D. E. Shaw Research: New York, NY, 2017.
- (46) Li, P.; Roberts, B. P.; Chakravorty, D. K.; Merz, K. M., Jr. Rational Design of Particle Mesh Ewald Compatible Lennard-Jones

Parameters for +2 Metal Cations in Explicit Solvent. J. Chem. Theory Comput. 2013, 9, 2733-2748.

- (47) Zhu, F.; Hummer, G. Convergence and Error Estimation in Free Energy Calculations Using the Weighted Histogram Analysis Method. J. Comput. Chem. 2012, 33, 453-465.
- (48) Roux, B. The calculation of the potential of mean force using computer simulations. Comput. Phys. Commun. 1995, 91, 275-282.
- (49) Wang, W. J.; Park, R. Y.; Meyer, D. H.; Travesset, A.; Vaknin, D. Ionic Specificity in pH Regulated Charged Interfaces: Fe³⁺ versus La³⁺. Langmuir 2011, 27, 11917-11924.
- (50) Bu, W.; Vaknin, D.; Travesset, A. How accurate is Poisson-Boltzmann theory for monovalent ions near highly charged interfaces? Langmuir 2006, 22, 5673-5681.
- (51) Sato, T. Liquid-Liquid Extraction of Rare-Earth Elements from Aqueous Acid Solutions by Acid Organophosphorus Compounds. Hydrometallurgy 1989, 22, 121-140.

□ Recommended by ACS

Theoretical Insights into the Selectivity of Hydrophilic Sulfonated and Phosphorylated Ligands to Am(III) and Eu(III) Ions

Yao Zou, Wei-Qun Shi, et al.

MARCH 09, 2023

INORGANIC CHEMISTRY

READ **'**

Selective Extraction of Critical Metals from Spent Lithium-**Ion Batteries**

Mengmeng Wang, Daniel C. W. Tsang, et al.

FEBRUARY 17, 2023

ENVIRONMENTAL SCIENCE & TECHNOLOGY

READ 🗹

Lanthanide and Actinide Ion Complexes Containing Organic Ligands Investigated by Surface-Enhanced Infrared **Absorption Spectroscopy**

Sakiko Hirata, Yoshiya Inokuchi, et al.

DECEMBER 22, 2022

INORGANIC CHEMISTRY

READ **C**

Aggregation Behavior of Nitrilotriacetamide (NTAmide) Ligands in Thorium(IV) Extraction from Acidic Medium: Small-Angle Neutron Scattering, Fourier Transform Infr...

Parveen K. Verma, Prasanta K. Mohapatra, et al.

NOVEMBER 17, 2022

LANGMUIR

READ **'**

Get More Suggestions >